ACS APPLIED NANO MATERIALS

www.acsanm.org Letter

Gold Nanoclusters Perform Enzyme-like Photocatalysis for Prodrug Activation

Rong Liu,[†] Dajiao Cheng,[†] Quan Zhou, Fushuang Niu, and Ke Hu*

Cite This: *ACS Appl. Nano Mater.* 2021, 4, 990–994 Read Online

ACCESS | Metrics & More | Article Recommendations | Supporting Information

ABSTRACT: Many synthetic nanomaterials known as nanozymes can catalyze biologically relevant molecular transformations just as natural enzyme does. "Photonanozyme" utilizes light as a spatial and temporal control for the regulation of nanozyme activities. Here we report a glutathione-modified gold nanocluster as a photonanozyme that catalyzes the reduction of nitrobenzene under light. Aniline was found as the sole photoreductive product. The photocatalytic reactions at variable light fluences were found to follow the classical Michaelis–Menten enzyme kinetics from which kinetic rate constants were quantified. Intracellular reduction of a nitro-group-containing fluorescent probe demonstrates the viability of gold nanoclusters as biocompatible photonanozymes performing catalysis in a mammalian cell environment. This study reinvents gold nanoclusters as photonanozymes that mimic naturally occurring nitroreductase for potential prodrug activation.

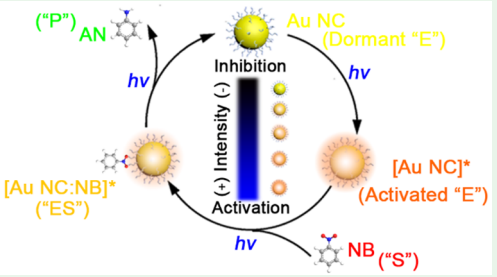

KEYWORDS: *gold nanocluster, photonanozyme, Michaelis–Menten enzyme kinetics, intracellular photocatalysis, prodrug activation*

Intracellular creation of biologically active molecules from prodrugs with catalytic nanomaterials is of great interest in biomedical applications such as *in vivo* imaging[1,2] and cancer therapy.[3−6] The ability to create such molecules with visible light would enable spatial and temporal control with an impact on these and emerging applications.[7−9] Here we report the initial development of *photonanozymes*, nanomaterials with enzyme-like catalytic properties that are activated with visible photons.

The photonanozyme is gold nanoclusters (Au NCs) of less than 2 nm diameter. They are shown to drive nitroreductase-like chemistry and reduce nitrobenzene to aniline. Unlike their larger plasmonic nanoparticle counterparts,[10,11] Au NCs possess discrete energy levels and long-lived photoluminescent (PL) excited states.[11,12] Hence, visible-light-absorbing Au NCs hold promise for the photocreation of biologically active molecules, but their photocatalytic behavior remains poorly documented. In this study, we have found that glutathione (GSH)-stabilized Au NCs perform photoinduced catalytic reduction of nitrobenzene to yield aniline as the only detected product. Aniline is an important moiety of a large class of synthetic molecular drugs that has previously been proposed to treat cancer in clinical trials, and its creation with light would be of considerable interest.[13] Scheme 1 shows that naturally occurring nitroreductase is a catalyst for nitrobenzene reduction with electrons from NAD(P)H, while the Au NCs perform the same reduction reaction with light and GSH as the electron source. We find that Au NC photonanozymes display light-fluence-dependent aniline production rates that follow classical Michaelis–Menten enzyme kinetics. As revealed by kinetic studies described herein, an advantage of these photonanozymes over natural enzymes or synthetic catalysts is that the aniline production rate can be fine-tuned with light. An extension of the photonanozymes to mammalian cells is also described.

Scheme 1. Comparative Illustration of Nitroreductase (Left) along with Au NC Photonanozyme (Right) Catalysis of the Prodrug Moiety Nitrobenzene to Biologically Active Aniline

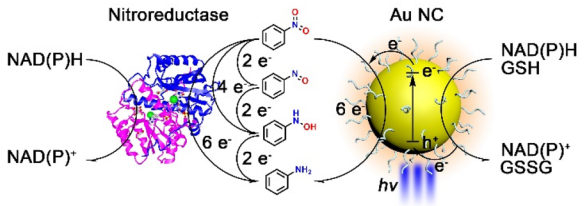

GSH-ligand-stabilized Au NCs were synthesized using a previously reported method.[14] Briefly, tetrachloroauric acid was mixed with GSH as the reductant in aqueous solution. Au NCs were allowed to grow at elevated temperatures, then purified by acetonitrile, and redispersed in deionized water. Electrophoresis showed an average GSH-ligand-stabilized Au NC weight of 14K g/mol (Figure S1). The as-synthesized Au

Received: January 3, 2021
Accepted: February 8, 2021
Published: February 12, 2021

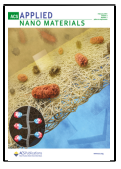

NCs showed visible-light absorption with an onset near 500 nm. Room temperature PL was observed with a maximum around 610 nm (Figure S2). Pulsed-light excitation of the Au NC resulted in time-resolved PL decays on a microsecond time scale. These optical features are consistent with literature reports of a 29−43 gold atom distribution of Au NCs.[14,15]

Photocatalytic nitrobenzene reduction was performed in anaerobic acidic solutions (pH = 1) with 450 nm light unless otherwise noted. Titration of nitrobenzene into the Au NC solutions resulted in PL quenching consistent with interfacial electron transfer from the photoexcited Au NC to nitrobenzene (Figure S3).

^{1}H NMR was employed to monitor the photocatalytic reduction of nitrobenzene. Aliquots taken every 15 min under steady-state illumination are shown in Figure 1. Aniline was the

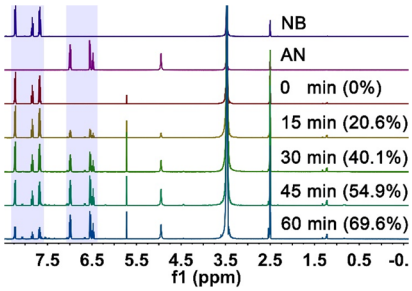

Figure 1. ^{1}H NMR analysis of photocatalytic nitrobenzene reduction at the indicated reaction time intervals with 0.14 mM Au NC and 0.1 M GSH with 1% (v/v) HCl (pH = 1) for complete dissolution in a 3/1 H_2O/methanol mixed solvent in a nitrogen gas environment under 450 nm illumination. Aniline conversion percentages are indicated in parentheses.

only product identified without unwanted nitrosobenzene or phenylhydroxyamine intermediates. Aniline as the sole photochemical product was also consistent with gas chromatography measurements, where no other reaction products were observed (Figure S4). Note that aniline was not observed in the absence of Au NCs or in the absence of light (Figure S5). Neutral pH or aerobic conditions decreased the reaction rate but not the composition of products (Figures S6 and S7). In addition, spherical plasmonic Au nanoparticles of much larger 5−8 nm diameter[16] were incompetent of nitrobenzene photoreduction (Figure S8), presumably because their short excited-state lifetimes precluded diffusional electron transfer.[17]

The creation of a single product is highly desirable and is a stark departure from previous work with photoexcited CdS quantum dots, where phenylhydroxylamine products were observed.[18] A clear explanation for why the Au NCs created a single reaction product while CdS did not is unknown. Previous enzymatic studies of nitro group reduction have revealed the presence of multiple catalytic pathways that are highly dependent on the enzyme structure.[19] In this regard, unique reaction mechanisms for CdS and Au might be anticipated. For these Au NC photonanozymes, consecutive two-electron reduction intermediates may have a high affinity for the Au surface, where they undergo six-electron reduction and the intermediates preclude detection. In other words, the partially reduced nitrobenzene intermediates may associate with the Au NC surface, where they are preferentially reduced to the final aniline product.

The enzyme mimetic reaction mechanism of photocatalytic nitrobenzene reduction was quantified by ultraviolet (UV) spectroscopy with 450 nm visible-light excitation. The conversion of nitrobenzene to aniline resulted in the bleaching of nitrobenzene absorption band centered at 260 nm, where aniline has minimal absorption (Figure S9a). The loss of nitrobenzene was quantified as a function of the irradiation time (Figure S9b). The initial reaction rate, r, was determined from the UV absorption change at the earliest time of the absorption measurement and plotted as a function of the nitrobenzene concentration, [S] (Figure S10). The initial reaction rate reached a maximum value when the nitrobenzene concentration exceeded a threshold value. This saturation behavior is reminiscent of natural enzyme catalysis, which often obeys the classical Michaelis−Menten mechanism. Indeed, Lineweaver−Burk plots (eq 1) of $1/r$ versus $1/[S]$ were linear (Figure 2) and allowed extraction of the maximum

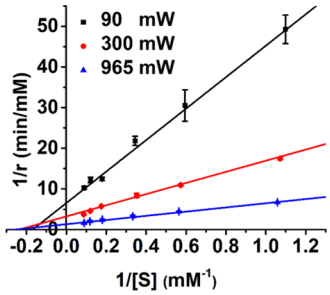

Figure 2. Lineweaver−Burk plot for nitrobenzene reduction by Au NC photonanozymes under the indicated 450 nm light fluence (8-mm-diameter illumination). Each data point is the average of three independent measurements. Overlaid is a linear fit.

catalytic rate (v_{max}), catalytic rate constant ($k_{cat} = v_{max}/[E]_0$, where $[E]_0$ is the total concentration of Au NC in units of millimolar), and catalytic efficiency (k_{cat}/K_M, where K_M is the Michaelis−Menten constant; Table 1). We note that nonlinear fits to the r versus [S] plots provided the same values within experimental error (Table S1).

$$\frac{1}{r} = \frac{1}{v_{max}} + \left(\frac{K_M}{v_{max}}\right)\frac{1}{[S]} \quad (1)$$

Table 1. Michaelis−Menten Constant (K_M), Maximum Catalytic Rate (v_{max}), Catalytic Rate Constant (k_{cat}), and Catalytic Efficiency (k_{cat}/K_M) at Variable Laser Fluences

$I_{450\ nm}$ (mW)	K_M (mM)	v_{max} (mM Min^{-1})	k_{cat} (min^{-1})	k_{cat}/K_M (mM^{-1} min^{-1})
90	5.9 ± 1.4	0.15 ± 0.02	0.52 ± 0.07	0.088 ± 0.033
300	4.2 ± 0.6	0.31 ± 0.02	1.1 ± 0.1	0.26 ± 0.06
965	3.9 ± 0.8	0.75 ± 0.08	2.6 ± 0.3	0.67 ± 0.21

Light-fluence-dependent data measured over a 965−90 mW range showed a marked rate dependence, as reflected in the slope and intercept of the Lineweaver−Burk plot (Figure 2 and Table 1). These kinetic data are critically important because they provide a means to experimentally predict the rate of aniline creation under steady-state illumination conditions.

The reduction mechanism of nitrobenzene or related nitroaromatic derivatives by thermocatalysis,[20,21] electrocatalysis,[22,23] or enzymatic catalysis[19] was widely studied in the past. The proposed mechanisms generally involve three sequential two-electron-transfer processes. The light-fluence-

https://dx.doi.org/10.1021/acsanm.1c00014
ACS Appl. Nano Mater. 2021, 4, 990−994

dependent behavior of the photocatalytic reduction of nitrobenzene by Au NC is significant in that light is identified as an experimental tool that regulates the catalytic turnover rate. We emphasize that light is critically required for the photonanozyme with no evidence for dark catalysis. Analogous to chemical inhibitors like dicoumarol or acetate that inhibit enzymatic nitroreduction,[24] light fluence can be used to control the rate of aniline production in these photonanozymes. Chemical inhibitors are generally inferior to light because they must be introduced into the sample and may initiate other unwanted chemistry.

As stated previously, these Au NC photonanozymes are not catalytically active and are hence dormant in the dark. Photon absorption activates the Au NC, as shown in the proposed catalytic cycle in Scheme 2. In the second step, nitrobenzene (NB) diffuses to the excited Au NC surface, where it is reduced with GSH present as an electron donor. A charge-separated state, designated as "ES", that undergoes at total of six electron transfers before the aniline (AN) product is released is then envisioned.

Scheme 2. Proposed Au NC Photonanozyme-Catalyzed Nitrobenzene Reduction Mechanism

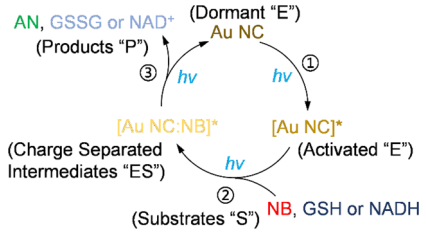

To understand the energetics of the proposed catalytic cycle, we note that the reduction potential of the photoexcited Au NCs was previously reported to be about −0.63 V versus normal hydrogen electrode (NHE).[25] The sequential two-electron-reduction potentials from nitrobenzene to aniline are reported to be −0.16, +0.29, and −0.46 V, with nitrosobenzene and phenylhydroxylamine as the two reduction intermediates.[18] Therefore, the Au NC photonanozymes are thermodynamically able to reduce nitrobenzene all the way to aniline.

Prior studies on nitroreductase detection by a fluorescent turn-on assay inspired a preliminary intracellular study of the Au NC photonanozymes.[1,26] To accomplish this, the fluorescent dye BODIPY was covalently linked to a nitrobenzene moiety, abbreviated as BODIPY-NB, and was tested in a fluid solution. The BODIPY fluorescence was quenched by nitrobenzene, as expected with a "turn on" when nitrobenzene was reduced. Indeed, light excitation of the Au NC showed the characteristic BODIPY fluorescence turn-on with a maximum near 502 nm (Figures S12 and S13).

With this BODIPY-NB probe tool in hand, viability tests of Au NC photonanozyme catalysis *in vitro* were initiated. Two cell lines, A549 and HeLa, showed high intake and low toxicity for the Au NCs (Figures S14 and S15). Confocal laser scanning microscopy (CLSM) showed low fluorescence upon 488 nm excitation, consistent with fluorescent quenching of BODIPY-NB. With 1−5 min of *in situ* 405 nm light excitation, the BODIPY fluorescence intensity from the cytoplasm was turned on and became stronger as illumination was continued. In comparison, the sample without Au NC incubation showed dim fluorescence over 5 min of irradiation (Figure 3a,c). The

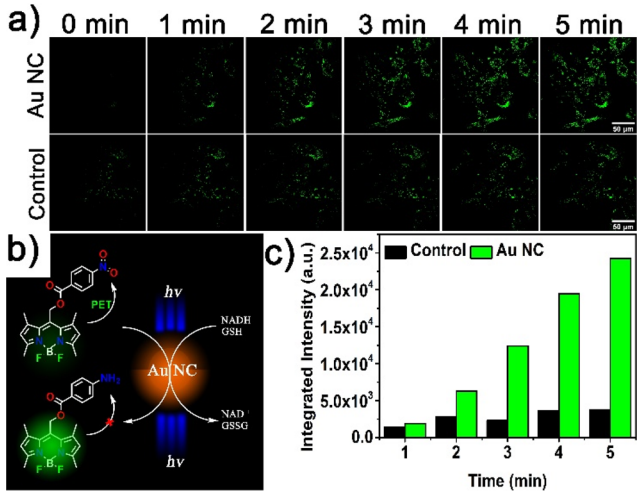

Figure 3. (a) CLSM images of A549 cells (λ_{ex} = 488 nm; λ_{em} = 505 ± 5 nm) incubated with Au NC and BODIPY-NB (upper row) and with BODIPY-NB alone as a control (lower row) under 405 nm laser irradiation from 0 to 5 min. (b) Molecular structure of BODIPY-NB and the proposed fluorescence turn-on mechanism upon photocatalytic reduction. (c) Whole image fluorescence intensity integration change of the control BODIPY-NB and BODIPY-NB with the Au NC photonanozymes from part a as a function of the irradiation time. Note that the background fluorescence from the probe itself at time zero was set to zero.

use of HeLa cells showed a similar fluorescence turn-on feature (Figure S16). The intracellular fluorescent turn-on result is consistent with the proposed photocatalysis mechanism from Scheme 2, where photoexcited intracellular Au NC catalyzes reduction of the nitrobenzene moiety to aniline (Figure 3b).

The question arose about which catalytic cofactor was involved in the intracellular redox environment. Costaining of the lysotracker or mitotracker with Au NC suggested that the photonanozymes were located within the lysosome where the photoreduction of the nitro group occurred (Figure S17). GSH is expected to be the major electron donor because the intracellular concentration is in the millimolar range and even up to 10 times more in cancer cells.

As a proof-of-concept application for photocatalytic drug activation, the photonanozymes were coincubated with CB1954, a prodrug for gene therapy under phase I clinical trials, and HeLa cells.[27] The phototoxicity of the Au NC was shown to be negligible (Figures S18 and S19). Illumination showed significant cytotoxicity with less than a 40% cell survival rate. In contrast, cells without the photonanozyme showed a much smaller effect (Figure S20). Note that CB1954 absorbs blue light, and this may complicate these cell viability tests. Nevertheless, to our knowledge, this is the first demonstration of a biomedical application of the Au NC photonanozyme.

In conclusion, gold nanoclusters were able to catalyze the challenging six-electron reduction of a prodrug moiety nitrobenzene to biologically active aniline under visible-light illumination. The light-fluence-dependent kinetics were shown to follow the classical Michaelis−Menten mechanism. This photoenzymatic catalysis behavior was regulated by the light fluence that could reversibly and remotely tune the aniline creation rate. A photonanozyme catalytic mechanism toward nitrobenzene reduction was proposed. This photoenzymatic reaction was able to occur in a complex intracellular

https://dx.doi.org/10.1021/acsanm.1c00014
ACS Appl. Nano Mater. 2021, 4, 990−994

environment, as evidenced by a nitro-group-containing fluorescent probe. This photocontrolled activation of a prodrug shows a clear advantage over traditional photodynamic therapy because it does not require oxygen. The proof-of-concept cellular studies open a new avenue for utilizing photo-nanozyme in biomedical applications such as directed enzyme prodrug therapy.

■ ASSOCIATED CONTENT

Supporting Information

The Supporting Information is available free of charge at https://pubs.acs.org/doi/10.1021/acsanm.1c00014.

Synthesis, experimental details, absorption, fluorescence and TEM data, additional data *in vitro*, and NMR spectra of relevant molecules (PDF)

■ AUTHOR INFORMATION

Corresponding Author

Ke Hu − *Department of Chemistry, Fudan University, Shanghai 200433, P. R. China;* orcid.org/0000-0002-0240-7192; Email: khu@fudan.edu.cn

Authors

Rong Liu − *Department of Chemistry, Fudan University, Shanghai 200433, P. R. China*

Dajiao Cheng − *Department of Chemistry, Fudan University, Shanghai 200433, P. R. China*

Quan Zhou − *Department of Chemistry, Fudan University, Shanghai 200433, P. R. China*

Fushuang Niu − *Department of Chemistry, Fudan University, Shanghai 200433, P. R. China*

Complete contact information is available at: https://pubs.acs.org/10.1021/acsanm.1c00014

Author Contributions

†These authors contributed equally.

Notes

The authors declare no competing financial interest.

■ ACKNOWLEDGMENTS

The authors thank the National Natural Science Foundation of China (Grant No. 21872037) for financial support. K.H. is particular grateful to Professor Gerald Meyer at University of North Carolina—Chapel Hill for helpful discussions on manuscript revision.

■ REFERENCES

(1) Li, Y.; Sun, Y.; Li, J.; Su, Q.; Yuan, W.; Dai, Y.; Han, C.; Wang, Q.; Feng, W.; Li, F. Ultrasensitive near-infrared fluorescence-enhanced probe for *in vivo* nitroreductase imaging. *J. Am. Chem. Soc.* **2015**, *137* (19), 6407−6416.

(2) Yu, F.; Li, P.; Wang, B.; Han, K. Reversible near-infrared fluorescent probe introducing tellurium to mimetic glutathione peroxidase for monitoring the redox cycles between peroxynitrite and glutathione *in vivo*. *J. Am. Chem. Soc.* **2013**, *135* (20), 7674−7680.

(3) Vong, K.; Yamamoto, T.; Chang, T.-c.; Tanaka, K. Bioorthogonal release of anticancer drugs via gold-triggered 2-alkynylbenzamide cyclization. *Chem. Sci.* **2020**, *11* (40), 10928−10933.

(4) Oliveira, B. L.; Stenton, B. J.; Unnikrishnan, V. B.; de Almeida, C. R.; Conde, J.; Negrao, M.; Schneider, F. S. S.; Cordeiro, C.; Ferreira, M. G.; Caramori, G. F.; Domingos, J. B.; Fior, R.; Bernardes, G. J. L. Platinum-Triggered Bond-Cleavage of Pentynoyl Amide and N-Propargyl Handles for Drug-Activation. *J. Am. Chem. Soc.* **2020**, *142* (24), 10869−10880.

(5) Vidal, C.; Tomas-Gamasa, M.; Gutierrez-Gonzalez, A.; Mascarenas, J. L. Ruthenium-Catalyzed Redox Isomerizations inside Living Cells. *J. Am. Chem. Soc.* **2019**, *141* (13), 5125−5129.

(6) Soldevila-Barreda, J. J.; Metzler-Nolte, N. Intracellular Catalysis with Selected Metal Complexes and Metallic Nanoparticles: Advances toward the Development of Catalytic Metallodrugs. *Chem. Rev.* **2019**, *119* (2), 829−869.

(7) Zhang, J.; Liu, J. Light-activated nanozymes: catalytic mechanisms and applications. *Nanoscale* **2020**, *12* (5), 2914−2923.

(8) Alonso-de Castro, S.; Cortajarena, A. L.; Lopez-Gallego, F.; Salassa, L. Bioorthogonal Catalytic Activation of Platinum and Ruthenium Anticancer Complexes by FAD and Flavoproteins. *Angew. Chem., Int. Ed.* **2018**, *57* (12), 3143−3147.

(9) Gurruchaga-Pereda, J.; Martínez-Martínez, V.; Rezabal, E.; Lopez, X.; Garino, C.; Mancin, F.; Cortajarena, A. L.; Salassa, L. Flavin Bioorthogonal Photocatalysis Toward Platinum Substrates. *ACS Catal.* **2020**, *10* (1), 187−196.

(10) Stamplecoskie, K. G.; Kamat, P. V. Size-dependent excited state behavior of glutathione-capped gold clusters and their light-harvesting capacity. *J. Am. Chem. Soc.* **2014**, *136* (31), 11093−11099.

(11) Zhou, M.; Zeng, C.; Sfeir, M. Y.; Cotlet, M.; Iida, K.; Nobusada, K.; Jin, R. Evolution of Excited-State Dynamics in Periodic Au28, Au36, Au44, and Au52 Nanoclusters. *J. Phys. Chem. Lett.* **2017**, *8* (17), 4023−4030.

(12) Abbas, M. A.; Kamat, P. V.; Bang, J. H. Thiolated Gold Nanoclusters for Light Energy Conversion. *ACS Energy Letters* **2018**, *3* (4), 840−854.

(13) Williams, E. M.; Little, R. F.; Mowday, A. M.; Rich, M. H.; Chan-Hyams, J. V.; Copp, J. N.; Smaill, J. B.; Patterson, A. V.; Ackerley, D. F. Nitroreductase gene-directed enzyme prodrug therapy: insights and advances toward clinical utility. *Biochem. J.* **2015**, *471* (2), 131−153.

(14) Luo, Z.; Yuan, X.; Yu, Y.; Zhang, Q.; Leong, D. T.; Lee, J. Y.; Xie, J. From aggregation-induced emission of Au(I)-thiolate complexes to ultrabright Au(0)@Au(I)-thiolate core-shell nanoclusters. *J. Am. Chem. Soc.* **2012**, *134* (40), 16662−16670.

(15) Stamplecoskie, K. G.; Chen, Y.-S.; Kamat, P. V. Excited-State Behavior of Luminescent Glutathione-Protected Gold Clusters. *J. Phys. Chem. C* **2014**, *118* (2), 1370−1376.

(16) Chai, F.; Wang, C.; Wang, T.; Li, L.; Su, Z. Colorimetric detection of Pb2+ using glutathione functionalized gold nanoparticles. *ACS Appl. Mater. Interfaces* **2010**, *2* (5), 1466−1470.

(17) Kumar, A.; Kumar, S.; Kumari, N.; Lee, S. H.; Han, J.; Michael, I. J.; Cho, Y.-K.; Lee, I. S. Plasmonically Coupled Nanoreactors for NIR-Light-Mediated Remote Stimulation of Catalysis in Living Cells. *ACS Catal.* **2019**, *9* (2), 977−990.

(18) Jensen, S. C.; Bettis Homan, S.; Weiss, E. A. Photocatalytic Conversion of Nitrobenzene to Aniline through Sequential Proton-Coupled One-Electron Transfers from a Cadmium Sulfide Quantum Dot. *J. Am. Chem. Soc.* **2016**, *138* (5), 1591−1600.

(19) Mukherjee, A.; Rokita, S. E. Single Amino Acid Switch between a Flavin-Dependent Dehalogenase and Nitroreductase. *J. Am. Chem. Soc.* **2015**, *137* (49), 15342−15345.

(20) Wunder, S.; Polzer, F.; Lu, Y.; Mei, Y.; Ballauff, M. Kinetic Analysis of Catalytic Reduction of 4-Nitrophenol by Metallic Nanoparticles Immobilized in Spherical Polyelectrolyte Brushes. *J. Phys. Chem. C* **2010**, *114* (19), 8814−8820.

(21) Strachan, J.; Barnett, C.; Masters, A. F.; Maschmeyer, T. 4-Nitrophenol Reduction: Probing the Putative Mechanism of the Model Reaction. *ACS Catal.* **2020**, *10* (10), 5516−5521.

(22) Smith, W. H.; Bard, A. J. Electrochemical reactions of organic compounds in liquid ammonia. II. Nitrobenzene and nitrosobenzene. *J. Am. Chem. Soc.* **1975**, *97* (18), 5203−5210.

(23) Li, Y. P.; Cao, H. B.; Liu, C. M.; Zhang, Y. Electrochemical reduction of nitrobenzene at carbon nanotube electrode. *J. Hazard. Mater.* **2007**, *148* (1−2), 158−163.

(24) Koder, R. L.; Miller, A. F. Steady-state kinetic mechanism, stereospecificity, substrate and inhibitor specificity of Enterobacter cloacae nitroreductase. *Biochim. Biophys. Acta, Protein Struct. Mol. Enzymol.* **1998**, *1387* (1−2), 395−405.
(25) Chen, Y. S.; Kamat, P. V. Glutathione-capped gold nanoclusters as photosensitizers. Visible light-induced hydrogen generation in neutral water. *J. Am. Chem. Soc.* **2014**, *136* (16), 6075−6082.
(26) Qi, Y.-L.; Guo, L.; Chen, L.-L.; Li, H.; Yang, Y.-S.; Jiang, A.-Q.; Zhu, H.-L. Recent progress in the design principles, sensing mechanisms, and applications of small-molecule probes for nitroreductases. *Coord. Chem. Rev.* **2020**, *421*, 213460.
(27) Chung-Faye, G.; Palmer, D.; Anderson, D.; Clark, J.; Downes, M.; Baddeley, J.; Hussain, S.; Murray, P. I.; Searle, P.; Seymour, L.; Harris, P. A.; Ferry, D.; Kerr, D. J. Virus-directed, enzyme prodrug therapy with nitroimidazole reductase: a phase I and pharmacokinetic study of its prodrug, CB1954. *Clin. Cancer Res.* **2001**, *7* (9), 2662−2668.

https://dx.doi.org/10.1021/acsanm.1c00014
ACS Appl. Nano Mater. 2021, 4, 990−994